Numerical prediction of the detonation wave number

Qingyang Meng, Ningbo Zhao*, Hongtao Zheng, Jialong Yang, Lei Qi
College of Power and Energy Engineering, Harbin Engineering University
Harbin, Heilongjiang, China

1 Introduction

Rotating detonation combustor (RDC) has developed rapidly and emerged as a promising detonation-based combustor over the past few years due to its potential to realize higher efficiency and lower entropy production compared with traditional constant pressure combustor [1, 2]. Rotating detonation combustor generally confines the rotating detonation wave (RDW) with an annular cylindrical chamber consuming reactants fed continuously from the inlet at the head end of the chamber [3, 4]. The number of RDW is affected significantly by the equivalence ratio (φ) [5, 6], mass flow rate [7, 8] and inlet structure [9, 10]. Besides, different numbers of RDW show different propagating stability and performance, leading to that the combustor prefers certain number of RDW on particular working condition. Therefore, it is crucial to predict the number of RDW prior to the operation for the optimal performance of RDC. In current study, a three-dimensional numerical investigation is carried out to predict the number of RDW by considering the cell width, height of RDW and combustor width.

2 Numerical model

Figure 1 shows the computational domain and cross-section diagram of non-premixed RDC with slot-hole inlet structure. Air enters into combustor by a converging-diverging slot. Hydrogen is injected into a plenum firstly and then jet through holes. Ninety holes are evenly spaced on the inner wall. The hydrogen and air mixes like the jet-in-crossflow model. Different from the ideal premixed injection scheme, the non-uniform and stratified mixture is in front of the detonation wave. The specific geometric sizes about the computational domain are listed in Table 1.

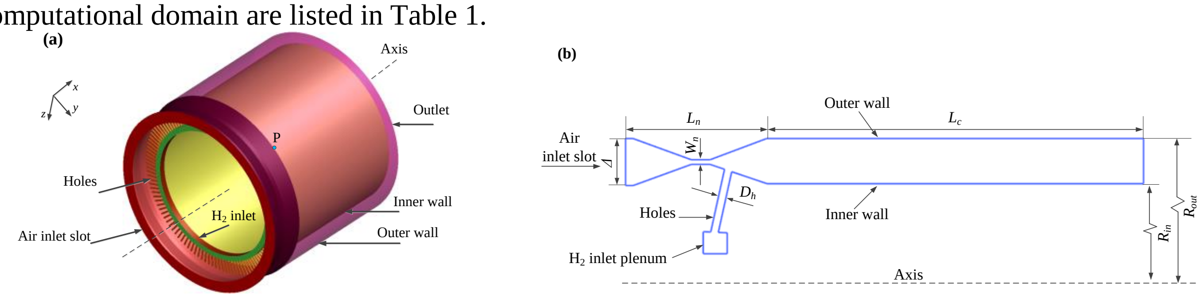

Figure 1. Schematic of RDC geometry (a): Computational domain; (b): Cross-section view

Correspondence to: zhaoningboheu@126.com

Table 1: Geometric sizes of combustor

L_n/mm	L_c/mm	Δ/mm	D_h/mm	W_n/mm	W_h/mm	R_{in}/mm	R_{out}/mm
15.0	40.0	5.0	0.8	0.6	0.8	35.0	40.0

3 Numerical methods and boundary condition Setup

All numerical results in current study are calculated by ANSYS Fluent. An unsteady Reynolds-Averaged Navier Stokes equation with hexahedral meshes (maximal size is 0.2mm) is used to simulate the formation and propagation of RDW on the basis of compressible flow. The time step size is selected as 2e^{-8}s. The two equations, k-ε turbulence model is employed to simulate the mixing process of air and hydrogen in combustor. Due to the existence of leading shock wave in RDW structure, the convective fluxes are calculated by Advection Upstream Splitting Method (AUSM) which performs excellent resolution of shock discontinuity. One-step chemical reaction is used here which produces reasonable results of RDW simulation [11-14]. The chemical reaction rate constant (k_f) is calculated by Arrhenius expression:

$$k_f = AT^b \exp(-E/RT) \tag{1}$$

where A denotes the pre-exponential factor, 1.03×10^9 s^{-1}. T is the temperature. b is the temperature exponent, 0. E is the activation energy, 1.26×10^5 J. R is the specific gas constant, 8.314 J/(mol K).

Table 2 shows the details of test cases. $\dot{m}_{\mathrm{H2}}$ is the mass flow rate of hydrogen, $\dot{m}_{\mathrm{air}}$ is the mass flow rate of air, $T_{\mathrm{H2/air}}$ is the total temperature of hydrogen and air, p_{b} is the back pressure, w_{ch} is the width of combustor. All the walls are treated to be adiabatic. In order to obtain the actual results especially the first cycle propagation of RDW, non-reacting simulation referring to mixing process is conducted before ignition. The ignition region simulates the kernel from pre-detonation tube of stoichiometric hydrogen-air possessing Chapman-Jouquet (CJ) parameters, pressure of 1.55MPa, temperature of 2942K and tangential velocity of 1964m/s. Note that the ignition direction is clockwise (from inlet to outlet view). Table 3 shows the comparison of detonation speed between numerical results and experimental data. It can be found that the deviations of velocity between numerical results and experiment are small enough, indicating the numerical methods can show reasonable results.

Table 2: Test parameters

Case	φ	$\dot{m}_{\mathrm{H2}}$ (kg/s)	$\dot{m}_{\mathrm{air}}$ (kg/s)	$\dot{m}_{\mathrm{total}}$ (kg/s)	$T_{\mathrm{H2/air}}$ (K)	p_{b} (MPa)	w_{ch} (mm)
#1	0.6	0.0018	0.10	0.1018	300	0.1	5.0
#2	0.8	0.0024	0.10	0.1024	300	0.1	5.0
#3	1.0	0.0030	0.10	0.1030	300	0.1	5.0
#4	1.2	0.0036	0.10	0.1036	300	0.1	5.0
#5	1.4	0.0042	0.10	0.1042	300	0.1	5.0
#6	1.0	0.0021	0.07	0.0721	300	0.1	5.0
#7	1.0	0.0030	0.10	0.1030	300	0.1	8.0
#8	1.0	0.0030	0.10	0.1030	300	0.1	12.0

Table 3: Comparison of velocity obtained by numeric and experiment

Case	Numerical (m/s)	Experimental (m/s) [15]	Error (%)
#3	1720	1680	2.3
#4	1956	1785	8.7

4 Results

4.1 Number of RDW

After ignition, the formation processes of RDW mainly experience the collision of detonation waves or transmit pressure waves and the re-initiation of reactant. Finally, self-sustaining detonation waves are established. Figure 2 shows the instantaneous pressure distributions of various cases when the stable RDW has been established. We can find that single wave for Case #4, #6, #7 and #8, while dual waves for Case #1, #2, #3 and #5. Note that the propagating direction of RDW in Case #1, #2 and #5 is opposite to the direction of ignition kernel, which is related to the collision of transmit pressure wave on RDW formation stage. Figure 3 shows the distributions of hydrogen ahead of RDW. For dual-wave mode (Case #1,2,3,5), as the increase of equivalence ratio, more hydrogen is observed but it close to the inner wall. By comparing Case #3 and #6, stratified hydrogen occurs obviously in Case #3. Besides, as the increase of annular width (Case #7 and #8), more hydrogen is close to the outer wall which might related to the wider space of combustor.

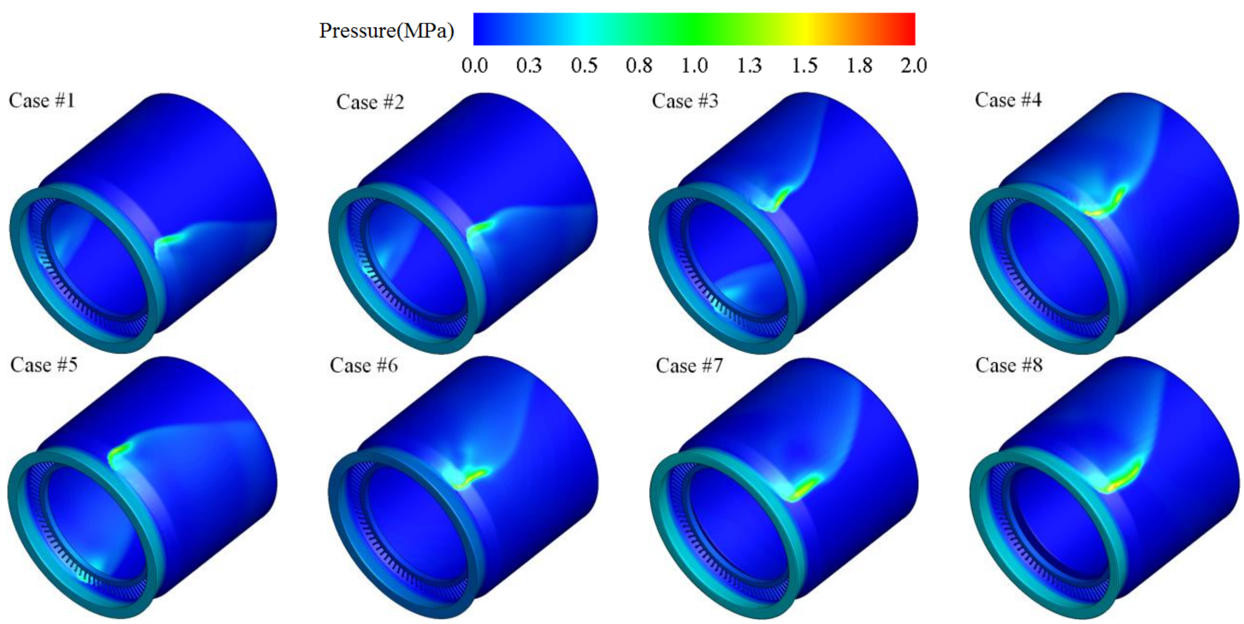

Figure 2. Contours of pressure

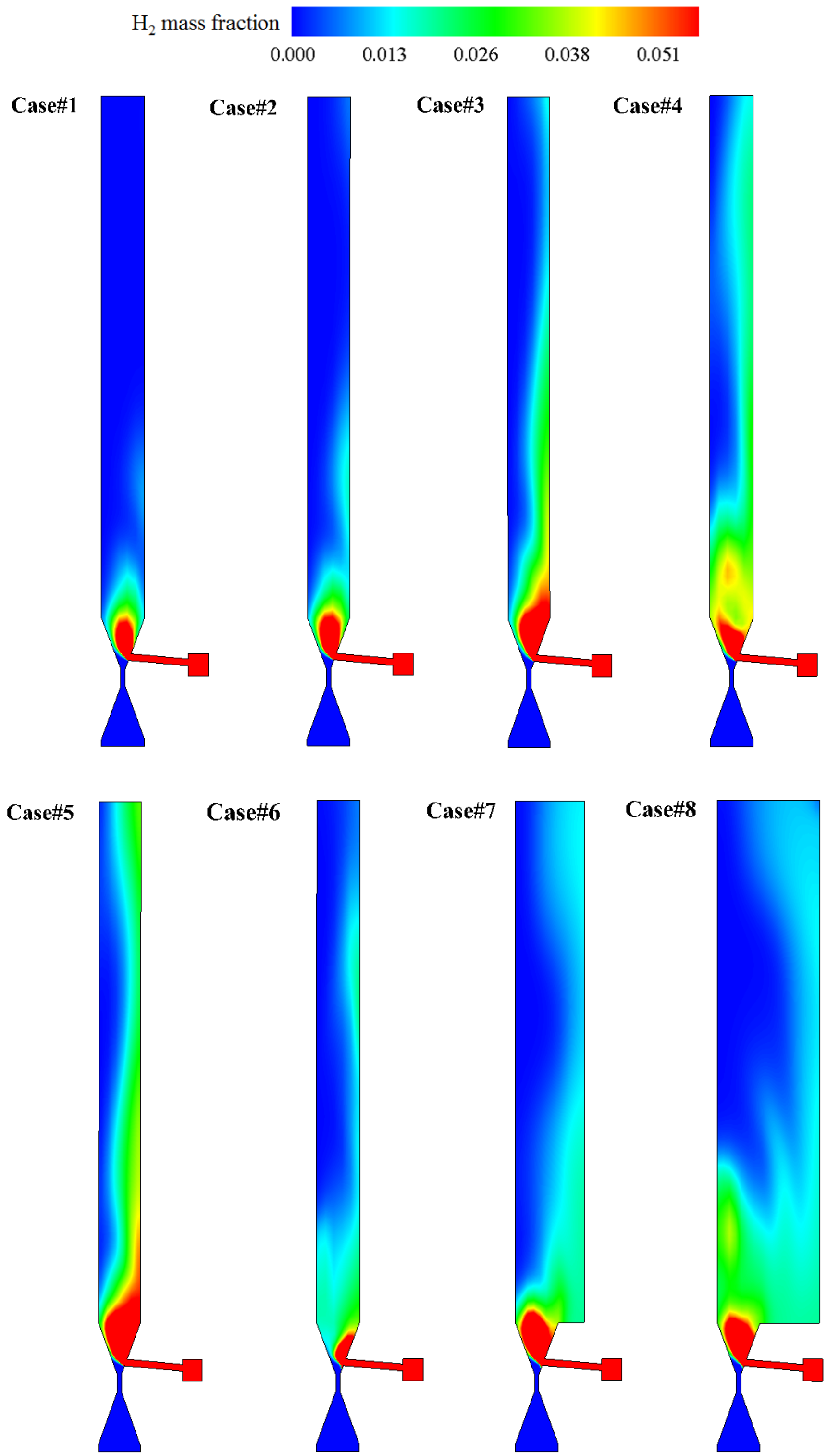

Figure 3. Distributions of hydrogen ahead of detonation wave

4.2 Prediction of detonation wave height and cell width

The global equivalence ratio is selected to calculate the cell width (λ). Limited by the accuracy of discrete scheme and the coarse grid, the cellular structure is not able to be observed. Referring to experimental results, Figure 4 plots the experimental data of cell width reported by Ciccarelli [16].

According to the conservation of mass and considering the incomplete combustion, the detonation wave height (h_{total}) is calculated by following formulas[16]:

$$h_{total} = \dot{m}_{total} \cdot (1 - \alpha)/(\rho \cdot D \cdot w_{ch}) \tag{2}$$

$$p/\rho = R_g T \tag{3}$$

where h_{total} means the summary height of each indivisual RDW, $\dot{m}_{\text{total}}$ is the total mass flow rate, α is the ratio of unburnt hydrogen to injectiong hydrogen from inlet, ρ is the reactant density, D is the speed of RDW, w_{ch} is the combustor width. p is the pressure, R_{g} is the gas constant which is obtained by the global equivalence ratio under different cases. It can be found that higher percentage of unburned reactant leads to lower height of RDW.

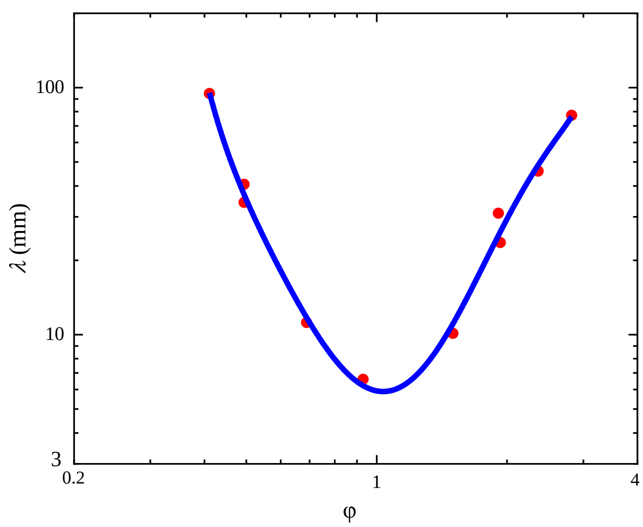

Figure 4. Polynomial fit of experimental data of cell sizes

4.3 Prediction of detonation wave number

The height of RDW and combustor width are normalized by cell width [17] and the combustion efficiency is also considered which has a great impact on the height of RDW. Table 4 lists the parameters dominating the number of RDW. Figure 5 shows the single-wave to dual-wave mode transition line and the distribution of the calculated cases. Note that the slope (k) of the transition line must be lower than 0, otherwise this unreal trend that dual-wave mode switches to single-wave mode when the detonation height is constant would occur as the cell width decreased. Besides, the smallest slope can be determined by Case #1 and Case #6. According to these two slopes, the range of the abrupt (b) is also calculated. Therefore, the transition line of single-wave to dual-wave transition boundary shows as following:

$$h_{total}/\lambda = k \cdot w_{ch}/\lambda + b \tag{4}$$

$$-0.57 < k < 0 \tag{5}$$

$$b > 2.16 \tag{6}$$

Table 4: Parameters of transition line

NO.	α(%)	ρ(kg/m^3)	D(m/s)	h_{total}/λ	w_{ch}/λ	mode
#1	11.2	0.37	1376.7	2.06	0.29	Dual
#2	9.5	0.61	1616.1	2.48	0.65	Dual
#3	2.5	0.61	1720.5	3.35	0.86	Dual
#4	3.0	0.89	1956.6	1.78	0.78	Single
#5	4.8	0.60	1803.9	2.08	0.57	Dual
#6	3.2	0.90	1755.2	1.52	0.86	Single
#7	8.6	0.91	1752.1	1.28	1.36	Single
#8	5.9	0.92	1750.3	0.88	2.04	Single

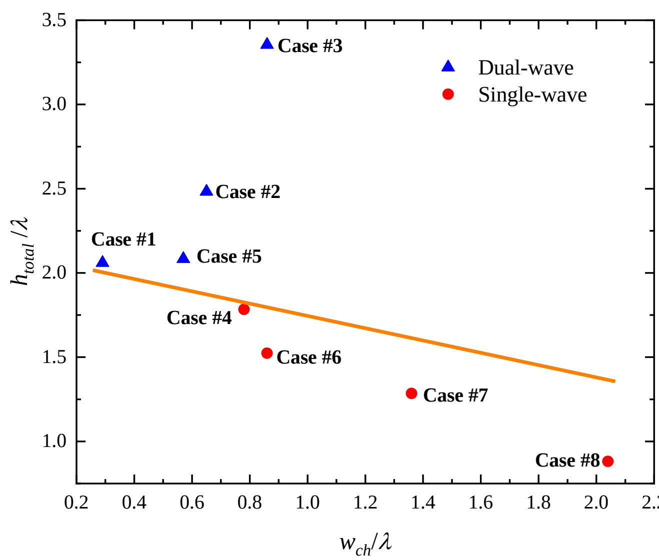

Figure 5. Relationship of transition line with test cases

5 Conclusion

Numerical results obtained from three-dimensional investigation of H_2/air rotating detonation combustor are presented in current study. Considering the combustion efficiency, the transition line of single-wave to dual-wave mode is obtained. The primary conclusions are drawn: (1) Low combustion efficiency reduces the height of RDW, leading the RDW easily locates in the single-wave mode region.(2) For current combustor, Case #4(φ=1.2, $\dot{m}_{total}$=0.1036kg/s, w_{ch}=5mm) are close to the transition line, indicating that it easily switches to dual-wave mode when the total mass flow rate increases. Similarly, Case #1(φ=0.6, $\dot{m}_{total}$=0.1018kg/s, w_{ch}=5mm) will switch to single-wave mode when the total mass flow rate decreases. (3) Limited by the computational expenditure, only eight cases are calculated in current study, resulting in the transition line is determined approximately within a certain range. More test cases need to be calculated to accurately describe the transition line in the future.

Acknowledgments

The authors would like to acknowledge the Fundamental Research Funds for the Central Universities (Grant No. HEUCFP201719) for supporting this work.

References

[1] Wolański P. (2013). Detonative propulsion. Proc. Combust. Inst. 34:125.

[2] Rankin BA, Fotia ML, Naples AG, Stenens CA, Hoke JL, Kaemming TA, Theuerkauf SW, Schauer FR. (2016). Overview of Performance, Application, and analysis of rotating detonation engine Technologies. J. Propul. Power. 33:1.

[3] Kindracki J. (2015). Experimental research on rotating detonation in liquid fuel-gaseous air mixtures. Aerosp. Sci. Technol.43:445.

[4] Sun J, Zhou J, Liu S, Lin Z, Lin W. (2018). Plume flowfield and propulsive performance analysis of a rotating detonation engine. Aerosp. Sci. Technol. 81:383.

[5] Li B, Wu Y, Weng C, Zheng Q, Wei W. (2018). Influence of equivalence ratio on the propagation characteristics of rotating detonation wave. Exp. Therm. Fluid Sci. 93:366.

[6] Masselot D, Fi´evet R, Raman V. (2017). Raman V. Effect of equivalence ratio and turbulence fluctuations on the propagation of detonations. 55th AIAA Aerospace Sciences Meeting.

[7] Qingyang M, Ningbo Z, Hongtao Z, Yang J, Qi L. (2018). Numerical investigation of the effect of inlet mass flow rates on H2 /air non-premixed rotating detonation wave. Int. J. Hydrogen Energ. 43:13618.

[8] Anand V, George AS, Driscoll R, Cutmark E. (2015). Characterization of instabilities in a rotating detonation combustor. Int. J. Hydrogen Energ. 40:16649.

[9] Katta VR, Cho KY, Hoke JL, Codoni JR, Schauer FR, Roquemore WM. (2018). Effect of increasing channel width on the structure of rotating detonation wave. Proc. Combust. Inst.8:37.

[10] Zhang H, Liu W, Liu S.(2016). Effects of inner cylinder length on H2/air rotating detonation. Int. J. Hydrogen Energ. 41:13281.

[11] Shao YT, Liu M, Wang JP. (2010). Numerical investigation of rotating detonation engine propulsive performance. Combust. Sci. Technol. 182:1586.

[12] Zhou R Wang JP. (2013). Numerical investigation of shock wave reflections near the head ends of rotating detonation engines. Shock Waves. 23:461.

[13] Wu D, Zhou R, Liu M, Wang JP. (2014) Numerical investigation of the stability of rotating detonation engines. Combust. Sci. Technol. 186:1699.

[14] Ma F, Choi JY , Yang V. (2006). Propulsive performance of airbreathing pulse detonation engines. J.Propul.Power, 22:1188.

[15] Anand V, George A S, Driscoll R, Gutmark E. (2016) Investigation of rotating detonation combustor operation with H2-Air mixtures. Int. J. Hydrogen Energ. 41:1281.

[16] Ciccarelli G, Ginsberg T, Boccio J, Economos KS, Kinoshita M. (1994). D etonation cell size measurements and predictions in hydrogen-air-steam mixtures at elevated temperatures. Combust. Flame. 99:212.

[17] George AS, Driscoll R, Anand V,Gutmark E. (2016). On the existence and multiplicity of rotating detonations. Proc. Combust. Inst.36:2691.